Applied Catalysis B: Environmental 245 (2019) 613–622

Contents lists available at ScienceDirect

Applied Catalysis B: Environmental

journal homepage: www.elsevier.com/locate/apcatb

A highly active and stable bimetallic Ni-Mo_2C catalyst for a partial oxidation of jet fuel

Qusay Bkour[a], Oscar G. Marin-Flores[a], M. Grant Norton[a,b,*], Su Ha[a,*]

[a] The Gene and Linda Voiland School of Chemical Engineering and Bioengineering, Washington State University, P.O. Box 646515, Pullman, WA, 99164-6515, USA
[b] School of Mechanical and Materials Engineering, Washington State University, P.O. Box 642920, Pullman, WA, 99164-2920, USA

ARTICLE INFO

Keywords:
Fuel reforming
Jet fuel
Molybdenum carbide
Isotope exchange
In-situ XRD

ABSTRACT

Mo_2C is an attractive catalyst for fuel reforming reactions because it possesses both a high activity and a high coking resistance. However, Mo_2C catalysts cannot guarantee sufficient long-term stability during fuel reforming reactions that operate at a high fuel flow rate due to their phase instability. The present investigation is focused on improving the phase stability and the performance of Mo_2C by addition of Ni for the partial oxidation (POX) of jet fuel. Mo_2C and Ni-Mo_2C were first prepared from CH_4/H_2 carburization of synthesized MoO_3 and $NiMoO_4$, respectively. To investigate the catalytic activity of carburized catalysts for the POX of jet fuel, tests were conducted at 750 °C and 1 atm, with a weight-hourly-space-velocity (WHSV) of 42 h^{-1} and O_2/C ratio of 0.6. The Mo_2C sample without Ni shows a performance similar to that of a blank run (in the absence of catalyst) with 70% conversion, 12% H_2 yield, and 53% CO yield. The poor performance of Mo_2C is due to its partial phase transformation into the MoO_2 phase at the high WHSV. For Ni-Mo_2C, the catalyst exhibits excellent stability over the 24 h test period with carbon conversion of 90% and H_2 and CO yields of 56 and 63%, respectively. There were no indications of bulk oxidation or surface coking. Temperature-programmed reaction and isotopic exchange experiments showed that Ni-Mo_2C follows the "catalytic oxidation and re-carburization cycle." In this cycle, molecular oxygen is activated over the Mo_2C surface, and the activated oxygen species react with lattice carbons from Mo_2C to produce both CO and carbon vacancies. Hydrocarbons are decomposed into H_2 and surface carbons over the metallic Ni sites. To sustain the catalytic cycle, the Mo_2C_{1-x} phase (i.e., non-stoichiometric Mo_2C with carbon vacancies) is re-carburized by the surface carbons deposited on the metallic Ni sites. Finally, our results also showed that $NiMoO_4$ can be rapidly carburized *in-situ* to form a high performance Ni-Mo_2C catalyst under a flowing mixture of *n*-dodecane and air.

1. Introduction

National energy security and global climate change concerns are greatly impacting future aircraft design, notably through the concept of the More Electric Airplane (MEA). MEA systems substitute hydraulic and pneumatic systems with electrical ones and replace the conventional low-efficiency gas turbine auxiliary power unit (APU) with a solid oxide fuel cell (SOFC) APU [1]. Fuel cells generate electrical power from the chemical energy of fuels in a cleaner and more efficient way than heat engines because they are not limited by the same thermodynamic constraints and produce much lower emissions than conventional generators [2–4]. However, the lack of a robust H_2 distribution infrastructure and the difficulty of hydrogen storage limits the effectiveness of SOFCs and has led to a focus onboard H_2 production from catalytic reforming of logistic liquid fuels such as kerosene-based aviation fuels, which are already present on commercial and military airplanes [5].

The reforming of logistic liquid fuels for fuel cell applications is a challenging proposition due to severe coking and sulfur poisoning issues. Therefore, the successful reforming of these hydrocarbons will largely depend on the development of new catalysts with much improved coking and sulfur poisoning resistances. Reforming of liquid fuels has been carried out over transition metal-based catalysts typically containing precious (noble) metals (e.g., Pd, Ru, Rh) [6–12]. Nevertheless, the high cost for even low loading of these noble metals prevents their widespread use. Ni-based catalysts are known as inexpensive catalytic materials for their liquid hydrocarbon reforming reactions. However, Ni sites rapidly deactivate due to severe coke formation [13].

* Corresponding authors at: The Gene and Linda Voiland School of Chemical Engineering and Bioengineering, Washington State University, P.O. Box 646515, Pullman, WA, 99164-6515, USA.
E-mail addresses: mg_norton@wsu.edu (M.G. Norton), suha@wsu.edu (S. Ha).

https://doi.org/10.1016/j.apcatb.2019.01.027
Received 7 September 2018; Received in revised form 28 December 2018; Accepted 9 January 2019
Available online 10 January 2019
0926-3373/

Transition metal carbides (TMCs) have attracted considerable attention because of their unique chemical and physical properties as well as their lower cost. TMCs have risen as prominent materials in heterogeneous catalysis and for the electro-catalysis of oxygen-containing species, which are likely related to strong carbide-oxygen interactions [14]. TMCs possess high electric and thermal conductivities. They are hard and have high melting temperatures [15]. It has been established that TMCs such as W and Mo have catalytic properties similar to those of noble metals [16]. Thus, TMCs show high activities in various catalytic reactions including: water gas shift [17–20], hydrogenation [21], desulfurization [22–24], CO_2 reduction [25,26], biomass conversion [27–30], and hydrocarbon isomerization [31].

Mo_2C is also an attractive catalyst for methane reforming because it does not require an excess of oxidant to operate without coke deposition [32–34]. Mo carbides have exhibited O_2 splitting activity similar to late transition metals, but with lower dissociation energy barriers [35]. It has been found that the stability of Mo_2C is strongly influenced by its tendency to transform into MoO_x under given redox environments [36]. Several studies have focused on the oxidation stability of Mo_2C during reforming reactions operated at atmospheric pressure at high temperature (> 950 °C) [37–40]. The Shi group focused on improving the stability of Mo_2C for methane reforming by doping it with Ni. They synthesized Ni-modified Mo_2C by temperature-programmed carburization of $NiMoO_x$ in a gas flow of CH_4/H_2 or CH_4/CO_2 [41]. The authors proposed that the rate of carburization of MoO_x is higher than Mo_2C oxidation over Ni-Mo_2C catalysts during methane dry reforming (MDR). Thus, Ni-Mo_2C catalysts maintained the carbide phase over the reaction time.

There are many other studies carried out on the performance of Mo_2C and its stability for methane reforming [32–34]. However, there have been very few published studies related to its performance and stability using liquid hydrocarbon fuels under reforming conditions. In 2006, the Thomson group [42] studied the feasibility of using Mo_2C as an efficient and inexpensive catalyst for the steam reforming (SR) and oxy-SR of 2,2,4-trimethylpentane (isooctane). They found that maximum hydrogen generation (85%) was observed at a steam/carbon ratio (S/C) of 1.3. Although the catalyst activity and stability were good, it was operated at a low space velocity (2 g of catalyst and gas-hourly-space-velocity GHSV = 1500 h^{-1}) and very high temperature (1000 °C). In 2008, Marin et al. [43] studied the performance of Mo_2C catalysts for isooctane SR. They found that a short H_2 pretreatment was needed to eliminate high oxidation states of Mo on the catalyst surface, namely oxycarbide Mo^{5+} and trioxide Mo^{6+}. Although the catalyst showed high activity at 850 °C and S/C of 1, it was also tested at a low weight-hourly-space-velocity (WHSV) of 1.8 h^{-1} and only initial performance was observed without long-term stability tests.

To the best of our knowledge, there are no published studies for either POX of jet fuel or SR of jet fuel at high space velocities over Mo_2C-based catalysts. In this work, Mo_2C and Ni-Mo_2C were prepared from CH_4/H_2 carburization of as synthesized MoO_3 and $NiMoO_4$, respectively. The catalytic reforming performances of samples were tested at a moderate temperature of 750 °C and a high WHSV of 42 h^{-1} for POX of both *n*-dodecane (model jet fuel) and actual jet fuel obtained from the local airport. In the present work, we also examined the feasibility of *in-situ* synthesis of Ni-Mo_2C (or Mo_2C) under the POX condition of *n*-dodecane from $NiMoO_4$ (or MoO_3). This work provides insight into the mechanism of the phase transformation of MoO_3 and $NiMoO_4$ into β-Mo_2C and Ni-Mo_2C, respectively, using *in-situ* XRD during the carburization reaction. In addition, in an attempt to explore the possibility of the redox mechanism for Ni-Mo_2C, which involves carbon exchange between pure hydrocarbons and carbide, we performed pulse isotopic exchange experiments with CH_4 over ^{13}C-labelled Ni-Mo_2C.

2. Experimental

2.1. Catalyst synthesis

We prepared $NiMoO_4$ using a combustion technique. For this, nickel nitrate $Ni(NO_3)_2.6H_2O$ (2.66 g), ammonium heptamolybdate (AHM) $(NH_4)_6Mo_7O_{24}.4H_2O$ (1.615 g), and glycine $C_2H_5NO_2$ (0.68 g) were dissolved in 50 ml distilled water separately and then combined to form a homogenous mixture. The mixture was then heated to 300 °C using a resistance heating furnace (Aroma, AHP-303). The resulting foamy powder was calcined at 500 °C for 4 h to obtain a single phase compound. MoO_3 and NiO were prepared as references using the same method with AHM and nickel nitrate precursors, respectively.

$NiMoO_4$ and MoO_3 were carburized in 20% CH_4/H_2 (66.7 mL/min) to Ni-Mo_2C and Mo_2C, respectively, through the following series of temperature-programmed processes: [1] the temperature was raised from room temperature to 300 °C in a span of 1 h [2], then increased from 300 to 700 °C at a rate of 1 °C min^{-1}, and [3] maintained at 700 °C for 2 h. The final material was cooled down to room temperature in flowing 20% CH_4/H_2 and passivated in a mixture of 2% O_2/Ar for 5 h.

2.2. Characterization

The crystalline phases of the catalytic materials were determined by X-ray diffraction (XRD) using a Rigaku (Miniflex 600) with Cu Kα radiation operated at 40 kV, 15 mA in steps of 0.01° with a scanning rate at 1 °C/min from 20° to 60°. Jade software was used for peak identification. Temperature-programmed carburization (TPC) studies were performed by loading 50 mg of the sample in a quartz tube reactor. The sample was preheated at 400 °C for 15 min under flowing Ar to remove adsorbed CO_2 and H_2O and cooled down to room temperature in flowing Ar. TPC profiles were obtained using a 5975C Agilent mass spectrometer with triple-axis detector with real-time gas analysis capability provided by Diablo Analytical. The sample was heated from room temperature to 750 °C at a rate of 10 °C/min in a flow of 20% CH_4/H_2 (67 mL/min) and maintained at 700 °C for 2 h. The signal intensity of H_2O (m/e = 18), CO (m/e = 28), H_2 (m/e = 2), CH_4 (m/e = 15), and CO_2 (m/e = 44) were monitored at a sampling rate of 1 s^{-1}. The reducibility of the samples was measured by temperature-programmed reduction (TPR): 100 mg of sample was placed in a quartz U-tube and pretreated with flowing He at rate of 50 mL/min. Following the pretreatment, 10%H_2/He was introduced at the same flow rate, while the temperature was ramped from 25 to 900 °C at a rate of 10 °C/min.

The catalytic partial oxidation (CPOX) of *n*-dodecane was performed in an isothermal fixed-bed tubular quartz reactor loaded with 50 mg of catalyst fixed in place by a quartz wool plug. A K-type thermocouple (Omega) was placed at the center of the catalyst bed to record and control sample temperature. Prior to the reaction, the passivated sample was reactivated with 20% CH_4/H_2 at 700 °C for 0.5 h. The reactant feed was composed of *n*-dodecane and air at an O_2/C ratio of 0.6 and was introduced to the reactor at WHSV of 42 h^{-1} at atmospheric pressure and 750 °C. Digital mass flow controllers and a syringe pump were used to control the flow rates of air and *n*-dodecane, respectively. The product stream was cooled to 5 °C to separate the condensable and gaseous products. The composition of the dry effluent gas (H_2, CO, CH_4, CO_2, C_2H_2 and C_2H_4) was analyzed by an SRI gas chromatograph equipped with molecular sieve 13X and HayeSep D packed columns and thermal conductivity detector. The conversion of *n*-dodecane during CPOX was calculated according to Eq. (1). The H_2 and CO yields were calculated according to Eqs. (2) and (3), respectively.

$$\%\,Conversion = \frac{moles\ of\ (CO + CO2 + CH4)\ produced}{12 * moles\ of\ n - dodecane\ fed} \quad (1)$$

$$\%\,H2\ Yield = \frac{2 * moles\ of\ H2\ produced}{26 * moles\ of\ n-dodecane\ fed} \quad (2)$$

$$\%\,CO\ Yield = \frac{moles\ of\ CO\ produced}{12 * moles\ of\ n-dodecane\ fed} \quad (3)$$

An oxygen pulsing experiment was conducted to seek direct evidence about the activation of O_2 over Mo_2C. In this experiment, 100 mg of Mo_2C was placed inside a quartz tube reactor and held by quartz wool. A flow of 50 sccm of ultra-pure argon was used to purge the reactor at room temperature for approximately 1 h, while 50 sccm of reactive gas (25% O_2 in Ar) was vented in parallel. Both streams entered separately into a 4-way pneumatic ball valve. After reaching the reaction temperature (750 °C), consecutive 5-s pulses of reactive gas were sent to the sample between 2 min purges of argon. Throughout the experiment, the concentration of the gases was monitored using a real-time gas analyzer mass spectrometer.

To conform the role of the lattice carbons present in the catalyst during the POX reaction, ^{13}C labelled Ni-Mo_2C (Ni-$Mo_2{}^{13}C$) was prepared and an isotope exchange study was performed. The Ni-$Mo_2{}^{13}C$ was prepared in a fixed bed reactor, in which $^{13}CH_4$ (50 mL/min) was fed to a $NiMoO_4$ sample at 700 °C. In the isotope exchange study, 50 mg of Ni-$Mo_2{}^{13}C$ was loaded into a quartz tube and heated to 750 °C under flowing He. Consecutive 5-s pulses of reactive gas (a gas mixture consisted of 8 mL/min $^{12}CH_4$ and 19.8 mL/min air with O_2/C of 0.5) were introduced to the catalyst at 750 °C and 1 atm between 2 min purges of He. The products were analyzed using on-line mass spectrometry.

3. Results and discussion

The XRD patterns of NiO, MoO_3, and $NiMoO_4$ are shown in Fig. 1 (A–C). Strong and sharp peaks attributable to NiO (2θ = 37.3 and 43.5°) corresponding to diffraction from the (111) and (200) crystal planes were observed in the NiO sample, which indicated the formation of a pure cubic NiO phase (bunesenite, NaCl type structure) [44]. The crystallite size of the prepared NiO, calculated from the XRD pattern using the Debye-Scherrer equation, is 26.9 nm. For the MoO_3 sample, the peaks at 2θ = 23.5, 25.7, 27.3, 29.8, 33.6, 35.5, 39.1, 46.3, 49.3, 52.7, 55.2, and 58.9° are attributed to the presence of orthorhombic (α-MoO_3 (JCPDS card No. 35-0609) [45]. The XRD pattern of $NiMoO_4$ shows the formation of the α-$NiMoO_4$ phase.

The XRD patterns for $NiMoO_4$ and MoO_3 after carbothermal treatment in a CH_4/H_2 gas mixture are shown in Fig. 1(D) and (E), respectively. Peaks at 2θ of 34.4, 38.0, 39.4 and 52.1° for the MoO_3 sample after the carbothermal treatment are assigned to the hexagonal β-Mo_2C phase. Both hexagonal β-Mo_2C and metallic nickel (2θ = 44.5, and 51.8°) are observed from the $NiMoO_4$ sample after the carbothermal treatment. No peaks corresponding to metallic molybdenum were observed from the $NiMoO_4$ sample after the carbothermal treatment [46,47]. The results indicated the complete carburization of MoO_3 and $NiMoO_4$ samples to form Mo_2C and Ni-Mo_2C, respectively. As calculated from the Ni diffraction peak at 44.5° for the Ni-Mo_2C sample, the Ni crystallite size was 23 nm.

The reducibility of NiO, $NiMoO_4$, and MoO_3 samples were studied via H_2-TPR (Fig. SI 1). As for NiO, one main reduction peak was observed at about 345 °C, which is ascribed to the reduction of NiO to metallic Ni [48,49]. The peak has a shoulder at around 410 °C, which can be assigned to the reduction of the larger particles [50]. The TPR profile of MoO_3 shows two distinct reduction peaks at around 700 and 865 °C. The sharp peak at 700 °C corresponds to the reduction of MoO_3 ($MoO_3 \rightarrow MoO_2$) and the peak at 820 °C is associated with the reduction of MoO_2 ($MoO_2 \rightarrow Mo$) [51]. A minor peak at around 720 °C can be ascribed to Mo_4O_{11} formed by reduction of MoO_3 ($MoO_3 \rightarrow Mo_4O_{11}$) [52–55]. For the $NiMoO_4$ sample, a minor reduction peak at 330 °C and two major peaks at 495 and 690 °C are observed. It is reported that $NiMoO_4$ partially decomposes into NiO and MoO_x under the H_2 reduction environment [56,57]. We believe that the reduction of NiO immediately occurred at the lowest temperature of 330 °C, while the reduction peaks at 495 and 690 °C are due to the reduction of MoO_x [16,58]. It is also noted that, compared with MoO_3 and NiO, the reduction of molybdenum in $NiMoO_4$ is easier as evidenced by the peak shifting to lower temperatures. It is clear that the presence of Ni has a substantial effect on the reduction of Mo oxide species due to interactions between Mo and Ni [41].

Fig. 2 displays the results of TPC obtained over MoO_3 and $NiMoO_4$ in a gas stream of 20%CH_4/H_2. In general, with the consumption of CH_4 (m/e = 15) there is clear production of both CO (m/e = 28) and H_2O (m/e = 18) over the two samples. The consumption peak of H_2 (m/e = 2) is weak due to the poor sensitivity of H_2. In addition to this similarity in the TPC profiles of the two samples, they also show distinctly different characteristics. Over $NiMoO_4$, one can divide the profile into two regions. Below 500 °C, there is a significant amount of H_2O formation with a small amount of CO formation, indicating that the reduction mainly takes place by H_2 rather than by CH_4 [16]. One can deduce that there is complete reduction of NiO to metallic Ni by H_2 below 500 °C. At temperatures higher than 500 °C, there is a large peak in CO generation accompanied by the formation of H_2O, which can be assigned to the carburization of MoO_x to Mo_2C at this higher temperature. The results are consistent with the H_2-TPR observation that the H_2 reduces $NiMoO_4$ to both Ni metal and MoO_x at temperatures

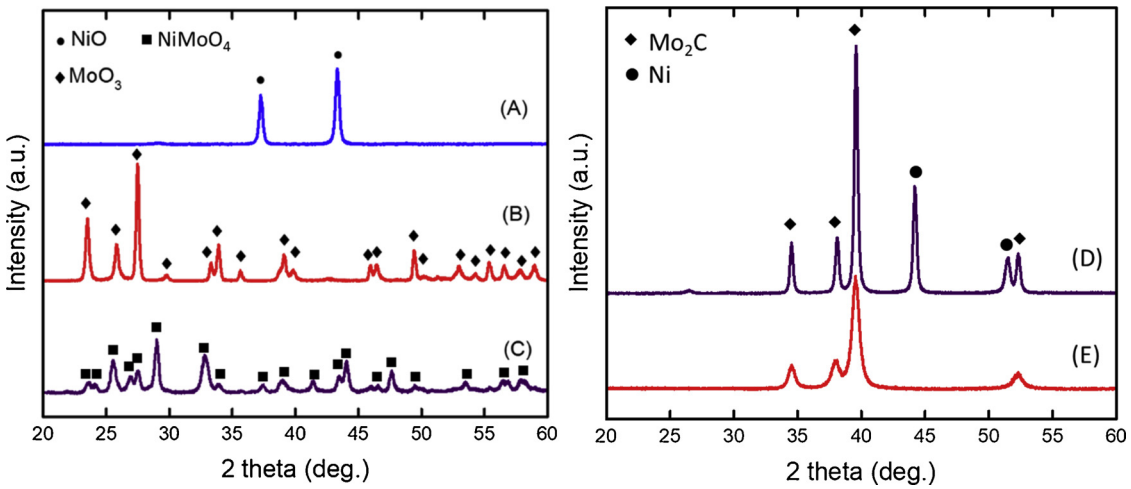

Fig. 1. XRD patterns of NiO (A), MoO_3 (B), $NiMoO_4$ (C) Ni-Mo_2C (D), and Mo_2C (E). The carbide samples were formed after carburization of oxide samples using 20% CH_4/H_2 in N_2 carrier gas.

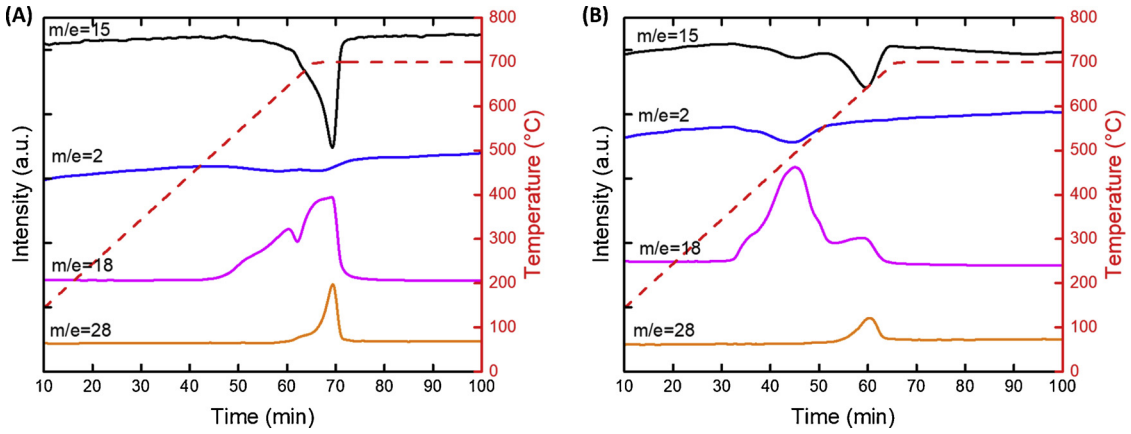

Fig. 2. 20% CH_4/H_2-TPC profiles of MoO_3 (A) and $NiMoO_4$ (B).

below 500 °C. At higher temperatures CH_4 dissociates over Ni to promote the MoO_x conversion into Mo_2C. It is worth noting that the carburization temperature for $NiMoO_4$ is 635 °C, while MoO_3 is carburized after reaching 700 °C and holding at temperature for 3 min. Based on CH_4/H_2 TPC results, we can deduce that the carburization of $NiMoO_4$ occurs at a lower temperature compared with MoO_3. It has been shown by other groups that the carburization temperature of MoO_x to Mo_2C is lowered by the presence of Ni and that $NiMoO_4$ is reduced at lower temperatures than those required for MoO_3 reduction [16,59–61].

In order to investigate the variation in the crystal phases of $NiMoO_4$ during the carburization process, a set of experiments were performed using *in-situ* XRD, which allows us to detect the appearance of new crystalline phases for any intermediates as the samples are exposed to 20%CH_4 in Ar at 750 °C. $NiMoO_4$ has two monoclinic atmospheric pressure isomorphs (space group C2/m) [62]: α-$NiMoO_4$ is octahedral and stable at room temperature, while β-$NiMoO_4$ is tetrahedral and formed by heating the α form above 690 °C [63]. Although both phases have differently coordinated Mo^{6+} ions, Ni^{2+} ions occur in sites with octahedral coordination in both cases. Mazzocchia et al. [64] found that at 590 °C, both phases coexist. However, a minimum temperature of 700 °C is required to obtain full conversion into the pure β phase. Our *in-situ* XRD analysis (Fig. SI 2) also indicates that at temperatures higher than 700 °C, the β phase is formed. Fig. 3 (A) shows the changes in the diffractogram of the $NiMoO_4$ while feeding 20%CH_4 in H_2. After a short time of feeding CH_4/H_2, the diffraction peaks due to β-$NiMoO_4$ disappeared and the diffraction peaks of MoO_2 and Ni appeared indicating that $NiMoO_4$ has been converted to MoO_2 and metallic Ni during the initial carburization process [41,65]. The MoO_2 peaks disappeared over time, while peaks of Mo_2C appeared without forming a metallic Mo phase.

The XRD results shown in Fig. 3 are consistent with the TPC observation that $NiMoO_4$ decomposes into NiO (which immediately reduces to Ni metal under the H_2 reducing condition) and MoO_2, and this Ni species enhance CH_4 dissociation to promote the further transformation of MoO_2 into Mo_2C. In summary, we propose that Reactions (1)–(5) occur in the carburization process. Based on the TPC results, MoO_2 can be carburized at higher temperatures than 500 °C to form Mo_2C via either Reaction (4) forming the CO_x species or Reaction (5) forming H_2O.

$$H_2 + NiMoO_4 \rightarrow NiO + MoO_2 + H_2O \quad (1)$$

$$NiO + H_2 \rightarrow Ni + H_2O \quad (2)$$

$$CH_4 + Ni^\circ \rightarrow Ni^\circ + C + 2\,H_2 \quad (3)$$

$$4\,C + 2\,MoO_2 \rightarrow Mo_2C + 2\,CO + CO_2 \quad (4)$$

$$C + 2\,MoO_2 + 4H_2 \rightarrow Mo_2C + 4H_2O \quad (5)$$

In-situ XRD was also performed using the pure MoO_2 phase without the presence of Ni. At the same CH_4 concentration used for the $NiMoO_4$ carburization, the MoO_2 phase was unchanged for the first 7 h (Fig. 3 (B)). The metallic Mo phase was detected after 6 h. The Mo_2C phase was detected after 9 h. The final result was a ternary solid oxide phase composed of MoO_2, Mo, and β-Mo_2C. Full carburization to Mo_2C was not achieved even after 10 h without the metallic Ni phase, which indicates that either (a) more time, (b) higher CH_4 concentration, or (c) higher temperatures are needed to complete the transformation. Ni metal therefore appears to be crucial in facilitating the dissociation of CH_4 to form the active carbon species, which is one of key steps for carburization. Without the sufficient amount of active carbons, the MoO_2 phase would be reduced to the metallic Mo phase instead of forming Mo_2C [20].

To investigate the catalytic activity of carburized catalysts for the POX of *n*-dodecane, we conducted their reforming tests at 750 °C and 1 atm, using a high WHSV of 42 h^{-1} and O_2/C ratio of 0.6, according to the following stoichiometric reaction:

$$C_{12}H_{26} + 6O_2 \rightarrow 12CO + 13H_2 \quad (6)$$

Fig. 4 shows the H2 yield, CO yield, and carbon conversion for the Ni, Mo2C, and Ni-Mo2C catalysts. For the Ni catalyst (after in-situ reduction of NiO with H2), there is a rapid deactivation along with a severe pressure drop due to the formation of carbon deposits on the surface of the catalyst, which can be seen in XRD data of its spent sample (Fig. 4 (D)). Mo2C (Fig. 4 (B)) has a performance similar to that of the blank run (in the absence of catalyst) with 12% H2 yield, 53% CO yield, and 70% conversion. The XRD data of spent Mo2C (Fig. 4 (E)) shows new diffraction peaks aside from the Mo2C peaks at 2θ of 26.0, 37.0, and 53.6° that are attributable to the MoO2 phase. This mixed phase is mainly responsible for the inactivity of Mo2C as shown in Fig. 4 (B). Under the POX reaction condition, molecular O2 would be easily activated over the pyrophoric Mo2C surface to form active oxygen species (O*), while the n-dodecane would decompose via the gas-phase reaction to create the various carbon fragments. These carbon fragments can be further reformed over the catalytic surface to form the surface carbon species. The active oxygen species can react with these carbon species to prevent surface coking. However, if the concentration of active oxygen species is higher than that of carbon species, Mo2C would be oxidized to form the catalytically inactive mixed phase. In the case of Mo2C without the metallic Ni phase, its ability to activate the carbon fragments into the surface carbon species would be limited. Consequently, the concentration of active oxygen species would be higher than that of the carbon species, which leads to the phase transition of Mo2C into oxide phases and the formation of the mixed phase. Unlike Mo2C, in the case of Ni-Mo2C (Fig. 4 (C)), the catalyst exhibits excellent activity and stability over the 24 h test period, showing carbon

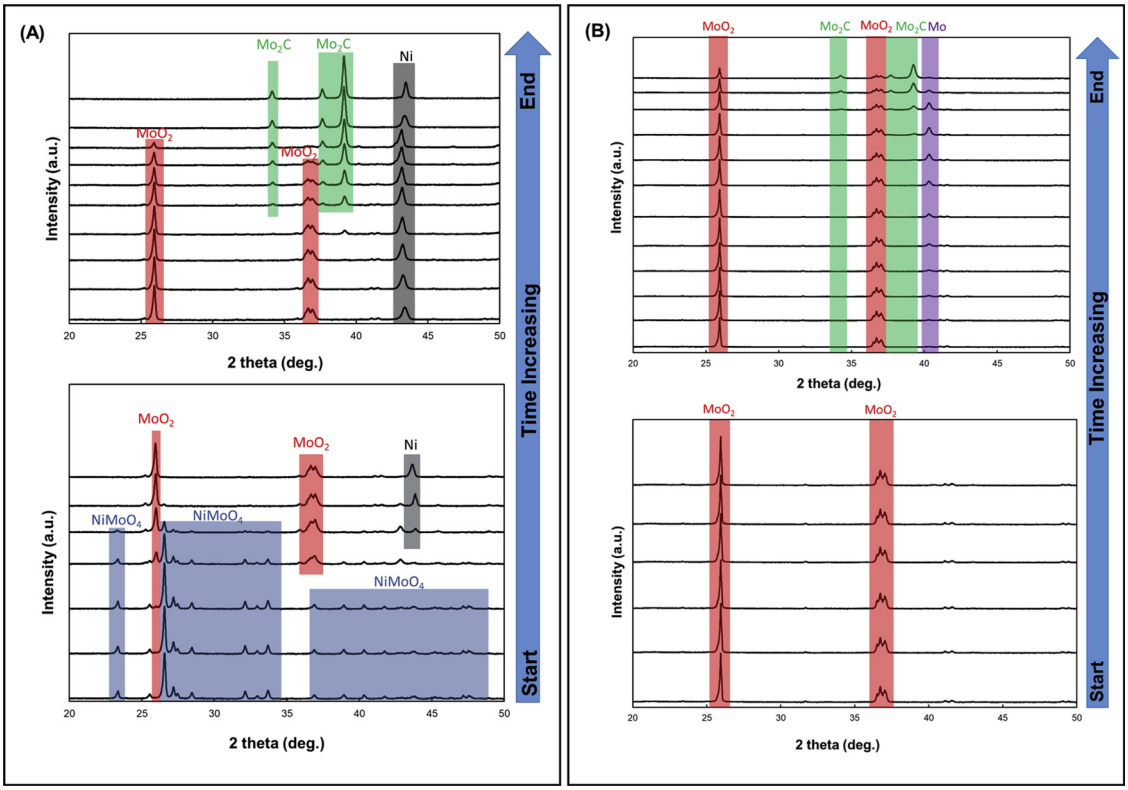

Fig. 3. *In-situ* XRD for the carburization process of $NiMoO_4$ (A) and MoO_2 (B) in 20% CH_4/H_2 at 750 °C. Start and End notations on the tail and top of the arrow correspond to the initial and final exposure time, respectively.

conversion around 90% with H2 and CO yields of 56 and 63%, respectively. XRD patterns of the spent Ni-Mo2C (Fig. 4 (F)) indicate only Mo2C and Ni phases. No oxides or coke deposits were detected. For Ni-Mo2C, the hydrocarbon fragments from the gas phase reaction can be more easily activated over Ni metal surfaces to form the surface carbon species, which can recarburize the MoOx to Mo2C [16,60,66]. In order words, the presence of metallic Ni can increase the stability of the Mo2C phase even at the high WHSV by increasing the rate of hydrocarbon activation and the surface carbon species concentration. We could not find any published papers investigating Mo2C-based catalysts for the POX of jet fuel. However, there are a few papers investigating the catalytic performance of Mo2C toward different reforming reactions or investigating the POX of jet fuel using different types of Mo-based catalysts. For example, Marin et al. [43] studied the performance of Mo2C catalysts for isooctane steam reforming. They found that a short H2 pretreatment was needed to eliminate high oxidation states of Mo on the catalyst surface, namely oxycarbide Mo5+ and trioxide Mo6 + . Although the catalyst showed high activity at 850 °C and S/C of 1, it was also tested at a low weight-hourly-space-velocity (WHSV) of 1.8 h-1 and only initial performance was observed without long-term stability tests. MoO2 particles was also investigated by Choi for POX of n-dodecane. It showed 60.8% of H2 yield and 87.4% of carbon conversion at low WHSV of 6.4 h-1 [67]. MoO2-based reforming systems exhibit optimum performance at low WHSVs due to the phase stability issue of MoO2, which leads to the low H2 production rate. For our current manuscript using a Ni-Mo2C catalyst, we were able to achieve both high H2 yield of 56% and high conversion of 90% at high WHSV of 42 h-1 for POX of n-dodecane. In order to achieve both high conversion and high H2 yield at the high WHSVs, the catalysts must be able to process a large volume of fuel per unit time. Our Ni-Mo2C catalyst can efficiently process the fuel at a WHSV of 42 h-1, which indicates that it possesses high catalytic activity compared to previously studied MoO2 catalysts under similar reforming conditions.

To further verify the role of metallic Ni for the POX reaction, the surface reaction of hydrocarbons (CH_4) over Mo_2C and Ni-modified Mo_2C catalysts was studied using CH_4-TPR. The CH_4-TPR was performed by loading 50 mg of the sample in a quartz tube reactor. The sample was preheated at 400 °C for 15 min under flowing Ar to remove adsorbed CO_2 and H_2O, and then it was cooled down to room temperature. The sample was heated from room temperature to 950 °C at a rate of 10 °C/min in flowing 10% CH_4/Ar (50 mL/min) and maintained at 950 °C for 30 min. Fig. 5 shows the results of CH_4-TPR experiments over the carbide samples in a gas stream of 10%CH_4/Ar. The consumption of CH_4 (along with the formation of CO, H_2, CO_2, and H_2O) was observed at 580 and 770 °C for Ni-Mo_2C and Mo_2C, respectively. These peaks are ascribed to an oxygen-assisted CH_4 oxidation to form CO and H_2. The oxygen source could be either the passivated carbide layers or the incomplete carburization of molybdenum oxide precursors (i.e., $NiMoO_4$ or MoO_3) [60,66]. Once all the surface oxygen species are consumed, the CH_4 can decompose into H_2 and elemental carbon at the high temperature if the catalysts are active for CH_4 activation. Only the Ni-Mo_2C sample showed this high temperature CH_4 activation at 950 °C, which indicates that the Mo_2C sample without Ni did not have sufficient CH_4 activity under the oxygen-deficient condition. Due to this poor activity of CH_4 activation, Mo_2C without Ni is oxidized by oxidizing agents (i.e., molecular O_2 or from CO_2 and H_2O reforming products) during POX and subsequently deactivates.

In the case of Ni-Mo_2C with the high hydrocarbon dissociation rate, there is an establishment of a “catalytic oxidation and re-carburization cycle” due to the synergistic effects between Mo_2C and metallic Ni. In this catalytic cycle shown in Fig. 6, the molecular oxygen is activated over the Mo_2C surface and the activated oxygen species react with lattice carbon of Mo_2C to form both CO and carbon vacancies (Reactions (7) and (8)). Hydrocarbons are decomposed into H_2 gas and surface carbons over the metallic Ni sites (Reaction (9)). To regenerate the Mo_2C phase and sustain the catalytic cycle, the Mo_2C_{1-x} phase (i.e., Mo_2C with the carbon vacancies) is re-carburized by the surface carbons deposited on the metallic Ni sites (Reaction (10)). By regulating

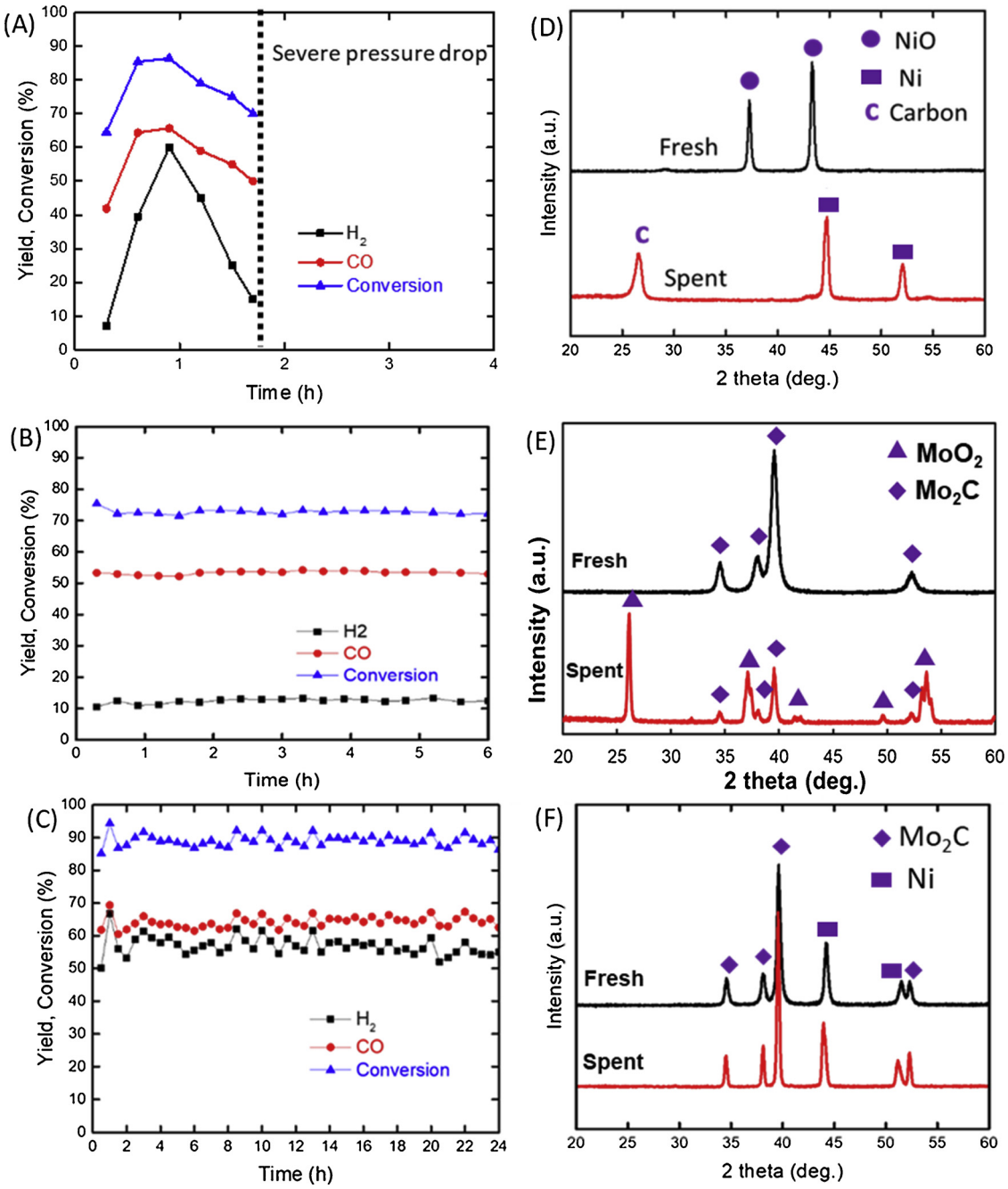

Fig. 4. Catalytic activity of Ni (A), Mo_2C (B) and Ni-Mo_2C (C) for partial oxidation of *n*-dodecane at temperature of 750 °C, O_2/C of 0.6 and WHSV of 42 h^{-1} and their XRD (D), (E), and (F), respectively.

the molar ratio of Ni and Mo_2C, a catalytic oxidation-recarburization cycle could be established and the net oxidation of carbides could be avoided [60].

$$O_2 \overset{Mo_2C}{\Leftrightarrow} 2O^* \quad (7)$$

$$Mo\ [C]\ Mo + O^* \leftrightarrow Mo\ []\ Mo + CO + * \quad (8)$$

$$C_xH_y \overset{Ni}{\Leftrightarrow} x\,C^* + (y/2)H_2 \quad (9)$$

$$Mo\ []\ Mo + C^* \leftrightarrow Mo\ [C]\ Mo + * \quad (10)$$

An oxygen pulsing experiment was conducted to seek direct evidence about the activation of O_2 over Mo_2C. In this experiment, consecutive 5-s pulses of reactive gas (25% O_2 in Ar) were sent to the Mo_2C sample at 750 °C and 1 atm between 2 min purges of Ar. The gas product composition was analyzed as shown in Fig. SI 3. CO and CO_2 are detected as soon as the reaction starts due to the activation of O_2 over Mo_2C followed by the reaction of this activated oxygen with lattice carbons from Mo_2C (Reactions (7) and (8)). With time increasing, the concentrations of CO_2 and CO decrease with increasing O_2 concentration until the Mo_2C phase is completely converted into MoO_x, where there are no lattice carbons available to react with the activated oxygen. This oxygen pulsing experimental result clearly supports the high O_2 activation over Mo_2C.

We also prepared various physical mixture samples with different Ni/Mo_2C molar ratios. Fig. SI 4 (A) shows the XRD patterns of the as-prepared Ni/Mo_2C physical mixture samples. The peaks at 34.5, 38.1,

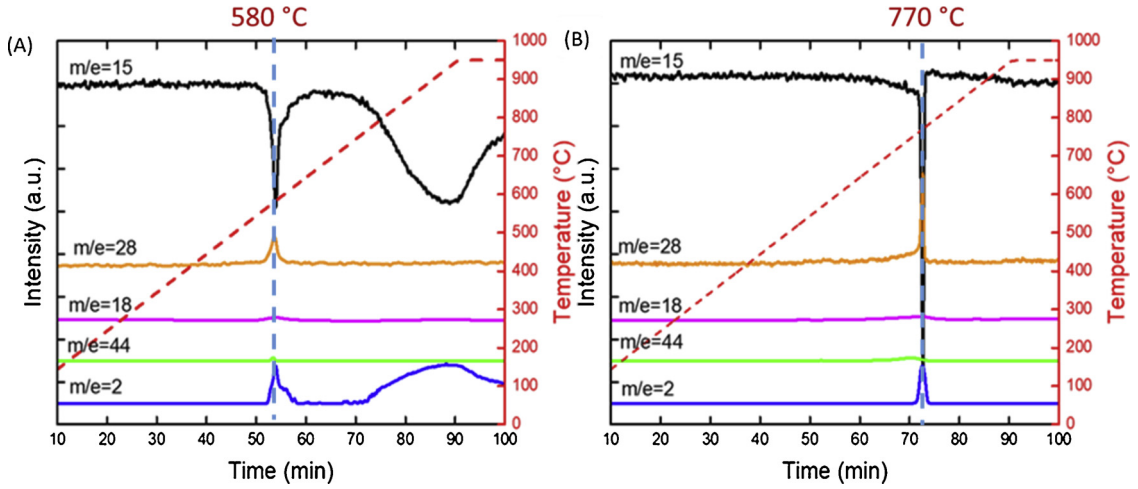

Fig. 5. CH_4-TPR profiles of (A) Ni-Mo_2C and (B) Mo_2C.

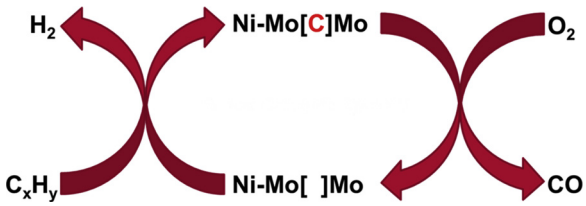

Fig. 6. Catalytic oxidation-reduction cycle over Ni-Mo_2C.

39.5, and 52.3° could be assigned to Mo_2C. In the case of Ni species, the peaks at 44.1 and 51.5° could be attributed to Ni metal, and these became more intense with increasing Ni/Mo molar ratio. The catalytic performance of Ni/Mo_2C physical mixture samples for POX of *n*-dodecane at 750 °C is shown in Fig. SI 5. The XRD data of the spent samples (Fig. SI 4 (B)) revealed that the deactivation of Ni-Mo_2C with a molar ratio of 0.5 was due to Mo_2C bulk oxidation whereas the deactivation of Ni-Mo_2C with a molar ratio of 5 was due to coke formation. At a Ni/Mo molar ratio of 1, the balance between catalyst oxidation and re-carburization could be established because the rate of O_2 activation matches the rate of hydrocarbon dissociation. Hence, coke formation and Mo_2C bulk oxidation are avoided.

Based on our proposed catalytic cycle shown in Fig. 6, the lattice carbon in Mo_2C catalysts acts as one of the key intermediate species for POX of hydrocarbons. To confirm the role of the lattice carbon for the POX reaction, ^{13}C labelled Ni-Mo_2C (Ni-$Mo_2{}^{13}C$) was prepared and an isotope exchange study performed. The Ni-$Mo_2{}^{13}C$ was prepared in a fixed bed reactor, in which $^{13}CH_4$ (50 mL/min) was fed to a $NiMoO_4$ sample at 700 °C (Fig. SI 6 shows the XRD of isotope-labeled catalyst).

In the isotope exchange study, 50 mg of Ni-$Mo_2{}^{13}C$ was loaded into a quartz tube and heated in flowing He to 750 °C. Consecutive 5-s pulses of reactive gas (8 mL/min $^{12}CH_4$ and 19.8 mL/min air mixture at O_2/C of 0.5) was introduced to the catalyst at 750 °C and 1 atm between 2 min purges of He. The products were analyzed using on-line mass spectrometry. The selectivity to isotope-labelled carbon oxide during the pulsing of the mixture of $^{12}CH_4/O_2$ is shown in Fig. 7. The relative intensity of ^{13}CO and ^{12}CO were 54% and 46%, respectively, for the first pulse over Ni-$Mo_2{}^{13}C$. Obviously, the ^{13}CO is produced from the oxidation of the lattice carbon in $Mo_2{}^{13}C$. This suggests that the lattice carbon in the carbide takes part in the reaction. The relative intensity of ^{13}CO decreased, while the ^{12}CO content increased for the second pulse. As pulsing continued, the yield of ^{13}CO continuously decreased, a result of the consumption of a fixed amount of the ^{13}C in the catalyst over time. Fig. SI 7 shows the XRD of the spent sample, indicating that bulk phase transformation did not occur. These results support our proposed reaction mechanism that the lattice carbon in the carbide catalyst is involved in the POX reaction as described in Fig. 6.

Conventionally, TPR of MoO_x in a gas flow of CH_4 and H_2 is used to prepare carbide catalysts [41]. To the best of our knowledge, there is no report on a direct *in-situ* synthesis of carbides in flowing *n*-dodecane/air at the reaction conditions. In this part of the work, we studied the feasibility for *in-situ* synthesis of Mo_2C and Ni-Mo_2C under the POX condition of *n*-dodecane from MoO_2 and $NiMoO_4$, respectively. The oxide was first heated from room temperature to 750 °C in a feed of N_2 gas, then a mixture of *n*-dodecane and air was introduced to the reactor at the same reforming conditions (O_2/C = 0.6 and WHSV = 42 h^{-1}). The sample was taken from the reactor after 30 min of feeding the *n*-dodecane/air mixture for further characterization. The XRD patterns of MoO_2 and $NiMoO_4$ catalyst after *in-situ* carburization in *n*-dodecane/air mixture are shown in Fig. 8.

In the case of MoO_2, the XRD pattern shows the peaks of MoO_2, indicating that Mo_2C cannot be synthesized *in-situ* during the POX reaction. When $NiMoO_x$ was used, only peaks attributable to Mo_2C and Ni metal are observed. These results indicate that $NiMoO_4$ could be carburized to Ni-Mo_2C in a flow of *n*-dodecane/air in a short time. The performance of the $NiMoO_4$ catalyst for the POX of *n*-dodecane was evaluated using the *in-situ* synthesis method of the carbide at 750 °C for 90 h (Fig. 9). The $NiMoO_4$ catalyst showed high activity and stability without any indication of oxidation or carbon formation, which was supported by the XRD pattern of the spent sample. These results confirm the possibility of utilizing the *in-situ* synthesis method of Ni-Mo_2C starting from $NiMoO_4$ without the need for a conventional temperature programmed reaction procedure, in which gaseous hydrocarbons and hydrogen are reacted over molybdenum oxide precursors at a slow heating rate over one day.

An additional test was performed to measure the activity of Ni-Mo_2C synthesized from the *in-situ* carburization method for the POX of actual jet fuel. As observed in Fig. 10, after 24 h of operation the catalyst remained stable with average H_2 and CO yields of 44% and 66%, respectively, and an average conversion of 90%. The blank run (without catalyst) showed H_2 yield, CO yield, and conversion of 2.5%, 53%, and 75%, respectively. For comparative purposes, Ni by itself showed a performance similar to that of the blank run with very severe coking. Fig. SI 8 showed that Ni-Mo_2C has relatively less coke formation than Ni when running POX of actual jet fuel at the high WHSV. Thus, based on these results, Ni-Mo_2C appears to cope well with the issues related to the use of aviation fuels, specifically coke formation.

4. Conclusion

In this work, Mo_2C and Ni-Mo_2C were synthesized from CH_4/H_2 carburization of previously prepared MoO_3 and $NiMoO_4$, respectively.

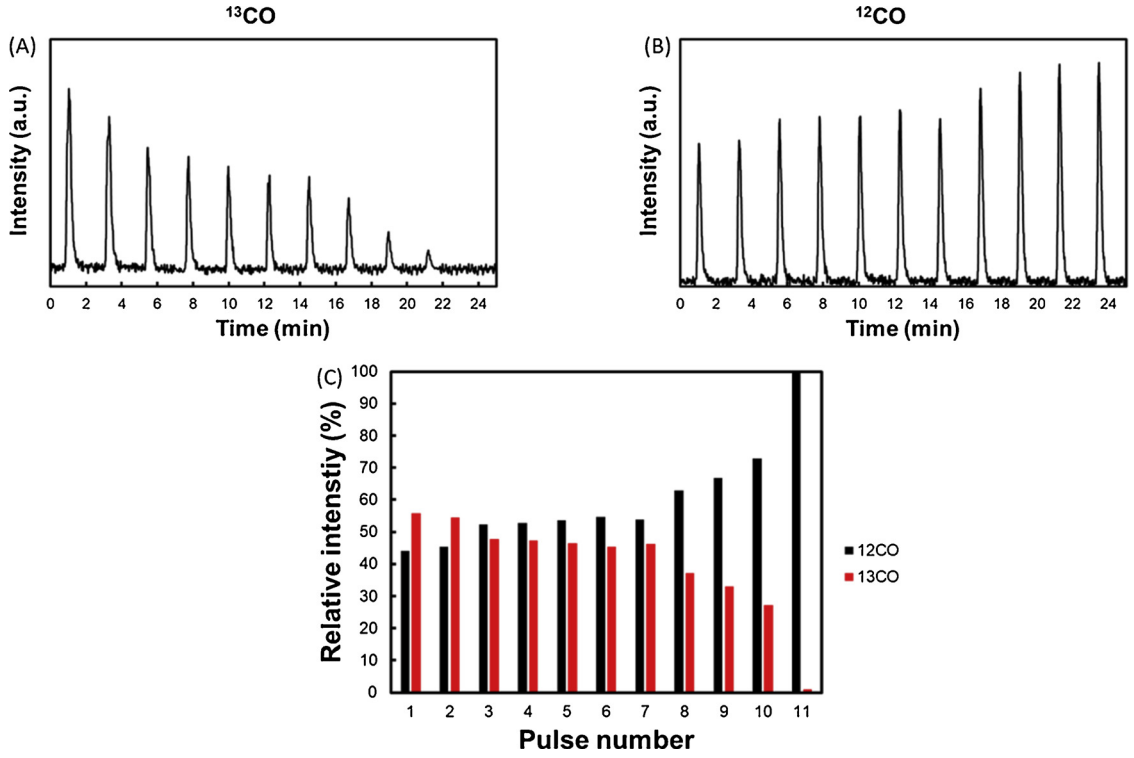

Fig. 7. Distribution of ^{12}CO and ^{13}CO as a function of pulse numbers. For each pulse, the mixture of $^{12}CH_4/O_2$ with a fixed volume was introduced to ^{13}C labelled Ni-Mo_2C (Ni-$Mo_2{}^{13}C$) at 750 °C and 1 atm.

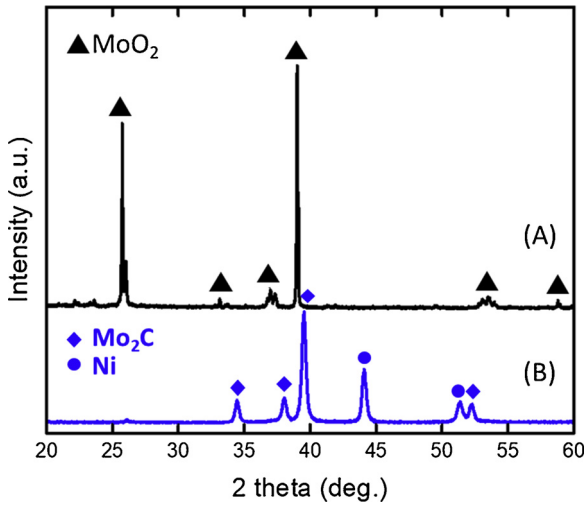

Fig. 8. XRD patterns of MoO_2 (A) and $NiMoO_4$ (B) after *in-situ* carburization in *n*-dodecane/air mixture at 750 °C for 30 min.

Our H_2-TPR results showed that compared with MoO_3 and NiO, the reduction of $NiMoO_4$ requires a lower energy as evidenced by the peak shifting to lower temperatures. It is clear that the presence of Ni has a substantial effect on the reduction of Mo oxide species. The CH_4/H_2-TPC results are consistent with the H_2-TPR observations that the H_2 decomposes and reduces $NiMoO_4$ to Ni metal and MoO_x at the lower temperature (below 500 °C). At higher temperatures than 500 °C, CH_4 dissociates over metallic Ni to promote the MoO_x conversion into Mo_2C. Based on CH_4/H_2-TPC results, the carburization temperature of MoO_x to Mo_2C is lowered by the presence of Ni.

In-situ XRD experiments were conducted to understand the phase transformation of MoO_2 and $NiMoO_4$ to β-Mo_2C and Ni-Mo_2C, respectively, during the carburization reaction. The results are consistent with the TPC observation that $NiMoO_4$ decomposes and reduces first to Ni metal and MoO_2 where the presence of Ni metal enhances hydrocarbon (CH_4) dissociation to promote the transformation of MoO_2 into Mo_2C. In the case of pure MoO_2, full carburization to Mo_2C was not achieved even after 10 h without the metallic Ni phase, which indicates that either (a) more time, (b) higher CH_4 concentration, or (c) higher temperatures were needed to achieve the complete phase transformation. Carburized materials were utilized as catalysts for the POX of *n*-dodecane at the high WHSV of 42 h^{-1}. Mo_2C showed a performance similar to that of the blank run (in the absence of catalyst) due to the partial transformation of the catalyst to the MoO_2 phase. On the other hand, Ni-Mo_2C catalyst exhibits the excellent performance over the 90 h test period, showing carbon conversion around 90% with H_2 and CO yields of 56 and 63%, respectively. The POX reaction over Ni catalysts (as reference) showed severe deactivation due to the formation of carbon deposits over the catalyst surface. The TPR and isotopic exchange experiments showed that Ni-Mo_2C follows the "catalytic oxidation and re-carburization cycle." In this catalytic cycle, molecular oxygen is activated over Mo_2C and these activated oxygen species react with lattice carbons to form both CO and carbon vacancies. Hydrocarbons are decomposed into H_2 gas and surface carbons over the metallic Ni sites. To regenerate the Mo_2C phase and sustain the catalytic cycle, the non-stoichiometric Mo_2C_{1-x} phase with carbon vacancies is re-carburized by the surface carbons deposited on the metal sites. Finally, our results indicated that Ni-Mo_2C can be prepared using *in-situ* carburization with a flowing *n*-dodecane/air mixture at 750 °C. The resulting product showed excellent POX performance toward *n*-dodecane and actual jet fuel.

Acknowledgement

This work was financially supported by the Office of Naval Research (Grant No. N00014-15-1-2416).

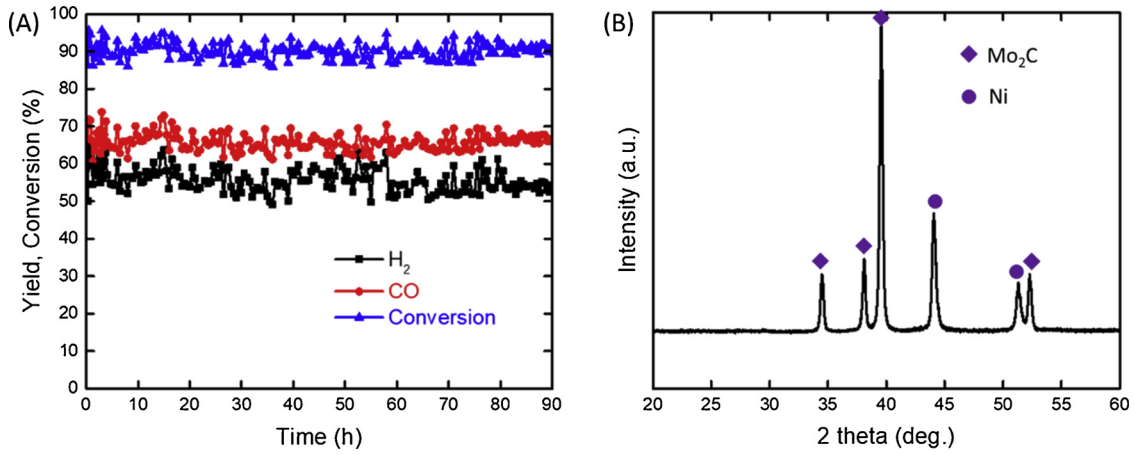

Fig. 9. Catalytic activity of Ni-Mo_2C (synthesized from the *in-situ* carburization using *n*-dodecane/air mixture) for the partial oxidation of *n*-dodecane at temperature of 750 °C and O_2/C of 0.6 (A) and its XRD data after the 90 h of the partial oxidation reaction (B).

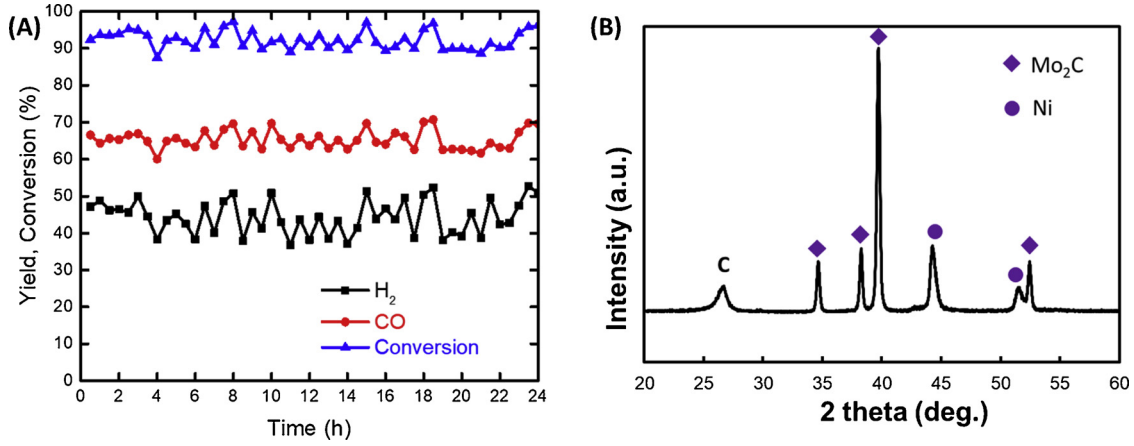

Fig. 10. Catalytic activity of Ni-Mo_2C (synthesized from the *in-situ* carburization using *n*-dodecane/air mixture) for the partial oxidation of actual jet fuel at temperature of 750 °C and O_2/C of 0.6 (A) and its XRD after the 24 h of the partial oxidation reaction (B).

Appendix A. Supplementary data

Supplementary material related to this article can be found, in the online version, at doi:https://doi.org/10.1016/j.apcatb.2019.01.027.

References

[1] O. Marin-Flores, T. Turba, C. Ellefson, K. Wang, J. Breit, J. Ahn, et al., Nanoparticle molybdenum dioxide: a highly active catalyst for partial oxidation of aviation fuels, Appl. Catal. B Environ. 98 (3–4) (2010) 186–192.

[2] O. Marin-Flores, T. Turba, C. Ellefson, L. Scudiero, J. Breit, M.G. Norton, et al., Sulfur poisoning of molybdenum dioxide during the partial oxidation of a Jet-A fuel surrogate, Appl. Catal. B Environ. 105 (1–2) (2011) 61–68.

[3] K. Zhao, X. Hou, Q. Bkour, M.G. Norton, S. Ha, NiMo-ceria-zirconia catalytic reforming layer for solid oxide fuel cells running on a gasoline surrogate, Appl. Catal. B Environ. 224 (2018) 500–507.

[4] K. Zhao, Q. Bkour, B.-H. Kim, M.G. Norton, S. Ha, NiMo-ceria-zirconia catalyst for inert-substrate-supported tubular solid oxide fuel cells running on model gasoline, Energy Technol. [Internet] (2018), https://doi.org/10.1002/ente.201700843 Available from:.

[5] P.K. Cheekatamarla, C.M. Finnerty, Synthesis gas production via catalytic partial oxidation reforming of liquid fuels, Int. J. Hydrogen Energy 33 (19) (2008) 5012–5019.

[6] W. Yanhui, W. Diyong, The experimental research for production of hydrogen from n-octane through partially oxidizing and steam reforming method, Int. J. Hydrogen Energy 26 (8) (2001) 795–800.

[7] R.P. O'Connor, E.J. Klein, L.D. Schmidt, High yields of synthesis gas by millisecond partial oxidation of higher hydrocarbons, Catal. Lett. 70 (3–4) (2000) 99–107.

[8] P.K. Cheekatamarla, A.M. Lane, Efficient bimetallic catalysts for hydrogen generation from diesel fuel, Int. J. Hydrogen Energy 30 (11) (2005) 1277–1285.

[9] P.K. Cheekatamarla, A.M. Lane, Catalytic autothermal reforming of diesel fuel for hydrogen generation in fuel cells: I. Activity tests and sulfur poisoning, J. Power Sources 152 (1–2) (2005) 256–263.

[10] J.J. Krummenacher, L.D. Schmidt, High yields of olefins and hydrogen from decane in short contact time reactors: rhodium versus platinum, J. Catal. 222 (2) (2004) 429–438.

[11] Q. Bkour, K. Im, O.G. Marin-Flores, M.G. Norton, S. Ha, J. Kim, Application of Ti-doped MoO2microspheres prepared by spray pyrolysis to partial oxidation of n-dodecane, Appl. Catal. A Gen. 553 (2018) 74–81.

[12] Q. Bkour, O.G. Marin-Flores, T.R. Graham, P. Ziaei, S.R. Saunders, M.G. Norton, et al., Nickel nanoparticles supported on silica for the partial oxidation of isooctane, Appl. Catal. A Gen. 546 (2017) 126–135.

[13] B.D. Gould, A.R. Tadd, J.W. Schwank, Nickel-catalyzed autothermal reforming of jet fuel surrogates: n-Dodecane, tetralin, and their mixture, J. Power Sources 164 (1) (2007) 344–350.

[14] W.-F. Chen, C.-H. Wang, K. Sasaki, N. Marinkovic, W. Xu, J.T. Muckerman, et al., Highly active and durable nanostructured molybdenum carbide electrocatalysts for hydrogen production, Energy Environ. Sci. 6 (3) (2013) 943.

[15] H.O. Pierson, Applications of refractory carbides and nitrides, Handbook of Refractory Carbides and Nitrides, (1996), pp. 309–326.

[16] C. Shi, S. Zhang, X. Li, A. Zhang, M. Shi, Y. Zhu, et al., Synergism in NiMoOx precursors essential for CH 4/CO2 dry reforming, Catal. Today 233 (2014) 46–52.

[17] J. Patt, D. Moon, C. Phillips, L. Thompson, Molybdenum carbide catalysts for water–gas shift, Catal. Lett. 65 (4) (2000) 193–195.

[18] P. Liu, J.A. Rodriguez, Water-gas-shift reaction on molybdenum carbide surfaces: essential role of the oxycarbide, J. Phys. Chem. B 110 (39) (2006) 19418–19425.

[19] H. Tominaga, M. Nagai, Density functional theory of water-gas shift reaction on molybdenum carbide, J. Phys. Chem. B 109 (43) (2005) 20415–20423.

[20] Qusay Bkour, Christian Martin Cuba-Torres, Oscar G. Marin-Flores, Shalini Tripathi, N. Ravishankar, M.Grant Norton, S.u Ha, Mechanistic study of the reduction of MoO2 to Mo2C under methane pulse conditions, J. Mater. Sci. [Internet] 53 (18) (2018) 12816–12827. Available from: https://link.springer.com/article/10.1007/s10853-018-2549-0.

[21] B. Dhandapani, T. St. Clair, S.T. Oyama, Simultaneous hydrodesulfurization, hydrodeoxygenation, and hydrogenation with molybdenum carbide, Appl. Catal. A Gen. 168 (2) (1998) 219–228.

[22] P. Da Costa, J.M. Manoli, C. Potvin, G. Djéga-Mariadassou, Deep HDS on doped molybdenum carbides: from probe molecules to real feedstocks, Catalysis Today,

(2005), pp. 520–530.
[23] J.A. Rodriguez, P. Liu, Y. Takahashi, K. Nakamura, F. Viñes, F. Illas, Desulfurization reactions on surfaces of metal carbides: photoemission and density-functional studies, Topics in Catalysis, (2010), pp. 393–402.
[24] P. Liu, J.A. Rodriguez, J.T. Muckerman, Desulfurization of SO 2 and thiophene on surfaces and nanoparticles of molybdenum carbide: unexpected ligand and steric effects, J. Phys. Chem. B 108 (40) (2004) 15662–15670.
[25] M.D. Porosoff, S. Kattel, W. Li, P. Liu, J.G. Chen, Identifying trends and descriptors for selective CO $_2$ conversion to CO over transition metal carbides, Chem. Commun. (Camb.) 51 (32) (2015) 6988–6991.
[26] M.D. Porosoff, X. Yang, J.A. Boscoboinik, J.G. Chen, Molybdenum carbide as alternative catalysts to precious metals for highly selective reduction of CO2 to CO, Ang. Chem. – Int. Ed. 53 (26) (2014) 6705–6709.
[27] J. Han, J. Duan, P. Chen, H. Lou, X. Zheng, H. Hong, Carbon-supported molybdenum carbide catalysts for the conversion of vegetable oils, ChemSusChem. 5 (4) (2012) 727–733.
[28] J. Han, J. Duan, P. Chen, H. Lou, X. Zheng, H. Hong, Nanostructured molybdenum carbides supported on carbon nanotubes as efficient catalysts for one-step hydrodeoxygenation and isomerization of vegetable oils, Green Chem. 13 (9) (2011) 2561.
[29] N. Ji, T. Zhang, M. Zheng, A. Wang, H. Wang, X. Wang, et al., Catalytic conversion of cellulose into ethylene glycol over supported carbide catalysts, Catal. Today 147 (2) (2009) 77–85.
[30] H. Ren, W. Yu, M. Salciccioli, Y. Chen, Y. Huang, K. Xiong, et al., Selective hydrodeoxygenation of biomass-derived oxygenates to unsaturated hydrocarbons using molybdenum carbide catalysts, ChemSusChem. 6 (5) (2013) 798–801.
[31] Y. Wang, H. Wang, M. Wei, J. Ma, Study on the isomerization of n-hexane over β-zeolite supported molybdenum carbide catalyst, Pet. Process Petrochem. 39 (2008) 16–19.
[32] H. Tominaga, M. Nagai, Theoretical study of methane reforming on molybdenum carbide, Appl. Catal. A Gen. 328 (1) (2007) 35–42.
[33] T. Christofoletti, J.M. Assaf, E.M. Assaf, Methane steam reforming on supported and non-supported molybdenum carbides, Chem. Eng. J. 106 (2) (2005) 97–103.
[34] D.C. Lamont, W.J. Thomson, Dry reforming kinetics over a bulk molybdenum carbide catalyst, Chem. Eng. Sci. 60 (13) (2005) 3553–3559.
[35] S. Politi JR dos, F. Viñes, J.A. Rodriguez, F. Illas, Atomic and electronic structure of molybdenum carbide phases: bulk and low Miller-index surfaces, Phys. Chem. Chem. Phys. 15 (30) (2013) 12617.
[36] D.C. LaMont, A.J. Gilligan, A.R.S. Darujati, A.S. Chellappa, W.J. Thomson, The effect of Mo2C synthesis and pretreatment on catalytic stability in oxidative reforming environments, Appl. Catal. A Gen. 255 (2) (2003) 239–253.
[37] David C. LaMont, J.Thomson William, The influence of mass transfer conditions on the stability of molybdenum carbide for dry methane reforming, Appl. Catal. A Gen. 274 (1) (2004) 173–178. Appl Catal A-GENERAL. 2004;274(1).
[38] A.J. Brungs, A.P.E. York, J.B. Claridge, M. Carlos, M.L.H. Green, Dry reforming of methane to synthesis gas over supported molybdenum carbide catalysts, Catal. Lett. 70 (2000) 117–122.
[39] S. Naito, M. Tsuji, T. Miyao, Mechanistic difference of the CO2 reforming of CH4 over unsupported and zirconia supported molybdenum carbide catalysts, Catalysis Today, (2002), pp. 161–165.
[40] A.R.S. Darujati, W.J. Thomson, Stability of supported and promoted-molybdenum carbide catalysts in dry-methane reforming, Appl. Catal. A Gen. 296 (2) (2005) 139–147.
[41] A. Zhang, A. Zhu, B. Chen, S. Zhang, C. Au, C. Shi, In-situ synthesis of nickel modified molybdenum carbide catalyst for dry reforming of methane, Catal. Commun. 12 (9) (2011) 803–807.
[42] P.K. Cheekatamarla, W.J. Thomson, Hydrogen generation from 2,2,4-trimethyl pentane reforming over molybdenum carbide at low steam-to-carbon ratios, J. Power Sources 156 (2) (2006) 520–524.
[43] O.G. Marin Flores, S. Ha, Study of the performance of Mo2C for iso-octane steam reforming, Catal. Today 136 (3–4) (2008) 235–242.
[44] N. Dharmaraj, P. Prabu, S. Nagarajan, C.H. Kim, J.H. Park, H.Y. Kim, Synthesis of nickel oxide nanoparticles using nickel acetate and poly(vinyl acetate) precursor, Mater. Sci. Eng. B Solid-State Mater. Adv. Technol. 128 (1–3) (2006) 111–114.
[45] L. Fang, Y. Shu, A. Wang, T. Zhang, Green synthesis and characterization of anisotropic uniform single-crystal α-MoO3 nanostructures, J. Phys. Chem. C 111 (6) (2007) 2401–2408.
[46] S. Zhang, C. Shi, B. Chen, Y. Zhang, Y. Zhu, J. Qiu, et al., Catalytic role of β-Mo2C in DRM catalysts that contain Ni and Mo, Catal. Today 258 (2015) 676–683.
[47] C. Shi, A. Zhang, X. Li, S. Zhang, A. Zhu, Y. Ma, et al., Ni-modified Mo 2C catalysts for methane dry reforming, Appl. Catal. A Gen. 431–432 (2012) 164–170.
[48] M. Broda, A.M. Kierzkowska, D. Baudouin, Q. Imtiaz, C. Copéret, C.R. Müller, Sorbent-enhanced methane reforming over a Ni-Ca-based, bifunctional catalyst sorbent, ACS Catal. 2 (8) (2012) 1635–1646.
[49] Qusay Bkour, Kai Zhao, Louis Scudiero, Chang Won Yoon, Oscar G. Marin-Flores, M. Grant Norton, S.u Ha, Synthesis and performance of ceria-zirconia supported Ni-Mo nanoparticles for partial oxidation of isooctane, Appl. Catal. B-Environmental. 212 (2017) 97–105.
[50] J. Sá, Y. Kayser, C.J. Milne, D.L. Abreu Fernandes, J. Szlachetko, Temperature-programmed reduction of NiO nanoparticles followed by time-resolved RIXS, Phys. Chem. Chem. Phys. 16 (17) (2014) 7692–7696.
[51] T. Bhaskar, K.R. Reddy, C.P. Kumar, Murthy MRVS, K.V.R. Chary, Characterization and reactivity of molybdenum oxide catalysts supported on zirconia, Appl. Catal. A Gen. 211 (2) (2001) 189–201.
[52] J.B. de Paiva Jr, W.R. Monteiro, M.A. Zacharias, J.A.J. Rodrigues, G.G. Cortez, Characterization and catalytic behavior of MoO3/V2O5/Nb2O5 systems in isopropanol decomposition, Brazilian J. Chem. Eng. 23 (04) (2006) 517–524.
[53] M. Alibouri, S.M. Ghoreishi, H.R. Aghabozorg, Hydrodesulfurization of dibenzothiophene using CoMo/Al-HMS nanocatalyst synthesized by supercritical deposition, J. Supercrit. Fluids 49 (2) (2009) 239–248.
[54] Y. Wang, G. Xiong, X. Liu, X. Yu, L. Liu, J. Wang, et al., Structure and reducibility of NiO-MoO3/γ-Al 2O3 catalysts: effects of loading and molar ratio, J. Phys. Chem. C. 112 (44) (2008) 17265–17271.
[55] K.V.R. Chary, T. Bhaskar, G. Kishan, K.R. Reddy, Characterization and reactivity of molybdenum oxide catalysts supported on niobia, J. Phys. Chem. B 105 (19) (2001) 4392–4399.
[56] J.L. Brito, A.L. Barbosa, Effect of phase composition of the oxidic precursor on the HDS activity of the sulfided molybdates of Fe(II), Co(II), and Ni(II), J. Catal. 171 (2) (1997) 467–475.
[57] L. Madeira, M. Portela, C. Mazzocchia, A. Kaddouri, R. Anouchinsky, Reducibility of undoped and Cs-doped α-NiMoO4 catalysts: kinetic effects in the oxidative dehydrogenation of n-butane, Catal. Today 40 (2–3) (1998) 229–243.
[58] J.L. Brito, a.L. Barbosa, Effect of phase composition of the oxidic precursor on the HDS activity of the sulfided molybdates of Fe (II), Co (II), and Ni (II), J. Catal. 171 (1997) 467–475.
[59] J. Cheng, W. Huang, Effect of cobalt (nickel) content on the catalytic performance of molybdenum carbides in dry-methane reforming, Fuel Process Technol. 91 (2) (2010) 185–193.
[60] J. Guo, A.J. Zhang, A.M. Zhu, Y. Xu, C.T. Au, C. Shi, A carbide catalyst effective for the dry reforming of methane at atmospheric pressure, ACS Symposium Series, (2010), pp. 181–196.
[61] T. HIROSE, Y. OZAWA, M. NAGAI, Preparation of a nickel molybdenum carbide catalyst and its activity in the dry reforming of methane, Chin. J. Catal. 32 (5) (2011) 771–776.
[62] A.W. Sleight, B.L. Chamberland, Transition metal molybdates of the type AMoO4, Inorg. Chem. 7 (8) (1968) 1672–1675.
[63] J.L. Brito, A.L. Barbosa, A. Albornoz, F. Severino, J. Laine, Nickel molybdate as precursor of HDS catalysts: effect of phase composition, Catal. Lett. 26 (3–4) (1994) 329–337.
[64] C. Mazzocchia, C. Aboumrad, C. Diagne, E. Tempesti, J.M. Herrmann, G. Thomas, On the NiMoO4 oxidative dehydrogenation of propane to propene: some physical correlations with the catalytic activity, Catal. Lett. 10 (3–4) (1991) 181–191.
[65] Y. Duan, R. Shang, X. Zhong, W. Xie, X. Wang, L. Huang, In-situ synthesis of Ni-Mo2C/Al2O3 catalysts for dry reforming of methane, Int. J. Hydrogen Energy 41 (47) (2016) 21955–21964.
[66] C. Shi, A. Zhang, X. Li, S. Zhang, A. Zhu, Y. Ma, et al., Ni-modified Mo2C catalysts for methane dry reforming, Appl. Catal. A Gen. 431–432 (2012) 164–170.
[67] H. Choi, D. Kim, S.P. Yoon, J. Han, S. Ha, J. Kim, Production of molybdenum oxide particles with high yield by ultrasonic spray pyrolysis and their catalytic activity toward partial oxidation of n-dodecane, J. Anal. Appl. Pyrolysis 112 (2015) 276–283.